19th Australasian Fluid Mechanics Conference
Melbourne, Australia
8-11 December 2014

Hypersonic Leading Edge Separation

A. Khraibut[1], N. R. Deepak[2], S. L. Gai[1], and A. J. Neely[1]

[1]School of Engineering and Information Technology
University of New South Wales, Canberra, ACT 2300, Australia

[2]Applied CCM Pty Ltd, Melbourne, Australia

Abstract

The case of leading edge separation at hypersonic speeds with moderate enthalpy flow conditions (Specific enthalpy, h_o = 3.1 MJ/kg, Mach number, M_∞ = 9.66, Reynolds number, Re_∞ = $1.3x10^6$ m^{-1}) is being investigated in this paper. To eliminate the complexity of a pre-existing boundary layer, a "tick" configuration is considered for a numerical study using an in-house Navier–Stokes based solver. A comparison between the Navier-Stoke results is made with a similar study using the Direct Simulation Monte Carlo method. The results are further used to test the applicability of Chapman's isentropic recompression theory at hypersonic conditions, which has not been done before. At the end of the study, the measured streamline angles at separation and reattachment are compared with Oswatitsch's formula relating angles at these locations with the shear stress and pressure gradients.

Introduction

The current research is part of University of New South Wales' (UNSW), Canberra, ongoing work to improve the understanding of hypersonic high-enthalpy flow separation experienced at high altitudes. Configurations such as compression corners, steps, and double-cones have been widely investigated for the past 20 years by UNSW at hypersonic speeds [4, 5, 7, 10], but they have the disadvantage of adding finite boundary layer thickness at separation into consideration. As a result, to avoid the problem of boundary layer development and simplify analysis, a "tick" configuration has been proposed by [3] is used in this study. Studying hypersonic flows over the "tick" configuration is also interesting from the physical point of view because it is considered as the limiting case of the base flow problem studied previously, and it is still not understood how the flow expansion at the leading edge affects the surface parameters or viscous layer/shock interactions.

A typical flow over a "tick" configuration is shown in figure 1. In general, the leading edge separation problem is characterized by a separation bubble caused by a strong expansion at **A** then followed by a recompression shock slightly downstream of reattachment at **C**. In theory, a constant pressure (p_d) exists in the region between **ABC**, also known as the recirculation region. Separating the outer inviscid flow and recirculation region is the viscous shear layer, which in theory defines p_d in the recirculation region. The "tick" configuration was used in this study to undergo a numerical investigation using a Navier–Stokes (N–S) solver especially developed for hypersonic flows. The results of the investigation were then directly compared to a study by [8] using the Direct Simulation Monte Carlo (DSMC) method. Parameters to be presented in the comparison are the locations of flow separation (**S**) and reattachment (**R**), which outline the separation bubble, and surface parameters critical to hypersonic applications such as the shear stress (τ_w), pressure (p/p_∞), and heat flux (q_w).

An important goal of the study is to test results from the N–S code against past separation theories proven successful in predicting p_d in the recirculation region such as the isentropic recompression theory developed by [3]. Chapman's theory has been validated in the past and shown to work remarkably well for a wide range of M_∞ and Re_∞ that experience laminar separation. The theory is especially attractive because it provides a very simple way of finding p_d by assuming an isentropic recompression at **R**, and a constant velocity ratio (u^*) along the shear layer. However, as the theory excludes the hypersonic regime, results from the N–S simulations will be applied into Chapman's theory to examine its applicability to the present hypersonic flow conditions.

The last part of the study is concerned with measuring the streamline angles at **S** and **R** and comparing them to a theoretical expression given by [9]. This will show whether a relationship between these streamline angles and the surface gradients exists.

Configuration and Flow conditions

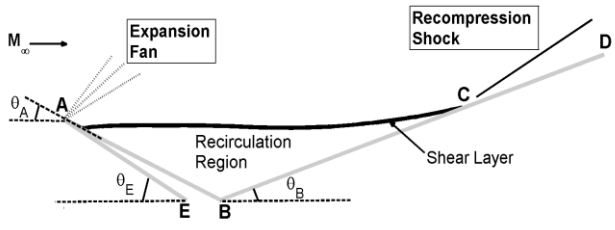

AB	BD	θ_A	θ_B	θ_E
19.7 mm	44.8 mm	-30.4°	23.7°	-42.3°

Figure 1: Geometry of "tick" configuration.

h_o MJ/kg	Re_∞ m^{-1}	U_∞ m/s	T_∞ K	ρ_∞ kg/m^3	p_∞ pa
3.1	$1.3x10^6$	2503	165	0.0061	288.9

Table 1: Freestream conditions.

The geometry of the "tick" model used for the study is shown in figure 1. The model has been developed to study leading separation at the same hypersonic conditions using the DSMC method. The flow conditions (Table 1) were produced at UNSW's T-ADFA shock tunnel by [5], and used for

simulations in [8] and the N–S simulations presented here. In table 1, U_∞, T_∞, ρ_∞, and p_∞ represent the freestream velocity, temperature, density and pressure, respectively.

Numerical Methodology

The numerical simulations were carried out using an in-house multi-block solver, Eilmer3. The code was specifically developed by [6] for hypersonic flows, and implements the cell-centered finite-volume discretization technique to obtain a time-accurate solution of the N–S equations. As an initial case, the operating fluid was assumed to be a calorically and thermally perfect air with the viscosity determined by Sutherland's formulation. The modified advection upstream splitting method (AUSMDV) was chosen as the flux splitting method for its robustness and accuracy in handling flow discontinuities such as shockwaves[13].

The leading edge was assumed to be infinitely sharp and taken as a baseline for later studies on the effects of the leading edge bluntness. To carry out the grid independence study, a set of three structured grids were developed and summarized in table 2.

Parameter	Coarse	Medium	Fine
i × j	207 × 44	414 × 88	828 × 176
Δs_w (μm)	20	20	20

Table 2: Summary of grids used in the study.

Grid refinement was achieved by simultaneously doubling the grid size in both i and j directions for both the medium and fine grids. The first cell height (Δs_w) was taken as 20 μm to sufficiently resolve the viscous layer and allow an economical simulation runtime.

As Eilmer3 is an explicit code, the time to reach steady-state was selected as the primary criterion to establish iterative convergence. The steady-state time was, therefore, monitored for surface parameters: τ_w, p/p_∞, and q_w. For the fine grid, a steady-state solution was achieved at 500 μs with time step (Δt) of the order of 10^{-10} s to maintain a CFL number of 0.5. The mesh and boundary conditions for the fine grid are shown in figure 2. The wall was held at a constant temperature of 288.9 K, and assumed to have no velocity slip or temperature jumps.

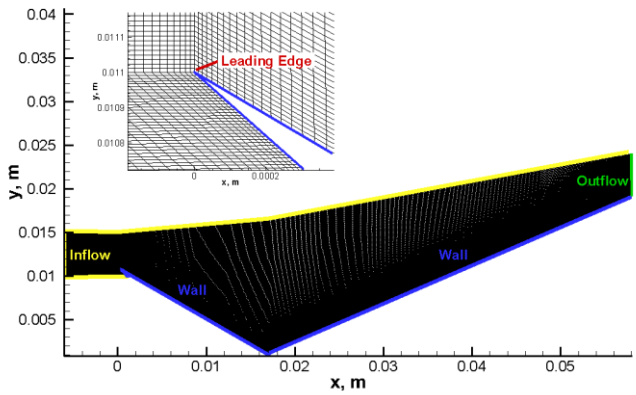

Figure 2: Mesh and boundary conditions for the coarse grid.

Results and Discussion

Grid Independence Study

The grid independence study is performed by calculating the grid convergence index (GCI) at the locations of **S** and **R** using the method described by [12]. The locations of **S** and **R** are determined from the distribution of τ_w as it crossed the zero line (Figure 3a). These locations are chosen as they define the separation region and have shown to be sensitive to mesh morphology. A good indication of grid convergence is seen in the consistent drop in both GCI_S and GCI_R with continuous grid refinement (Table 3). With GCI_S varying from 91.4% for the coarse grid to 0.8% for the fine grid, the location of **S** is found more sensitive to refinement than **R**. To conclude the grid independence study, the fine grid has been used for all subsequent analyses presented in the paper with sufficient confidence.

Grid	i × j	GCI_S (%)	GCI_R (%)
Fine	828 × 176	8.7	0.8
Medium	414 × 88	37.6	4.3
Coarse	207 × 44	91.4	7.7

Table 3: GCI values at separation and reattachment.

Comparison with DSMC

One of the primary goals of this study is to compare results of the N–S code with the DSMC results provided in [8]. Such comparison is crucial as both codes rely on different flow models: The N–S based on the continuum flow model, and the DSMC based on the real-time simulation of molecular collisions. As the continuum flow assumption breaks down at low densities, it is relevant to point out the flow conditions demonstrated in table 1 lie within the limits of the DSMC solver and N–S solver with no velocity slip condition. Consequently, a close agreement between the two fundamentally different codes was expected and will be demonstrated in the following results.

The locations of **S** and **R** obtained from both the N–S and DSMC solvers are shown in table 4. The locations are reported in terms of the normalized distance (s/Le), where s is the distance from the leading edge, and Le is the length of the expansion plate varying from s/Le = 0 at the leading edge to s/Le = 1 at the vertex.

For the location of **S** and **R**, table 4 shows a good agreement between the N–S and DSMC on the location of **R** in comparison to the location of **S**. For the size of the separation region (**R-S**), the DSMC predicts a 5% larger **R-S** possibly due to the earlier separation.

Code	S(s/L_e)	R(s/L_e)	R-S (s/L_e)
N–S	0.125	2.45	2.32
DSMC	0.08	2.51	2.43

Table 4: Separation and reattachment location.

Distributions of surface parameters τ_w, p/p_∞, and q_w in figure 3(a–c) further confirm the agreement between the N–S and DSMC solvers. Results from the DSMC code, however, show slightly larger peaks in surface parameters, possibly as a result of the bigger separated region. Interestingly, both codes show a consistent observation with previous studies by [4] in that the peak location of surface parameters occur slightly downstream of **R** in hypersonic flows. It is also interesting to note the

existence of a secondary vortex as indicated by the shear stress at the corner being positive instead of zero.

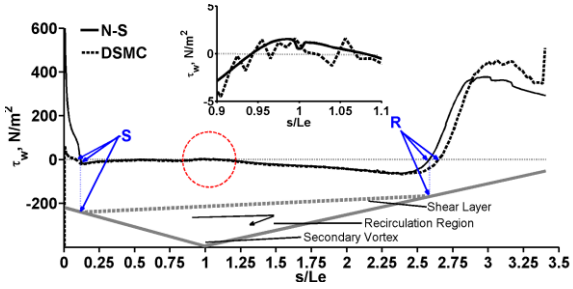

a) Surface shear stress.

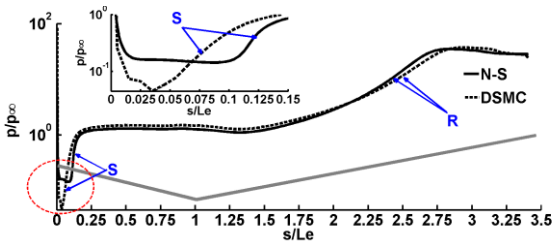

b) Surface pressure distribution.

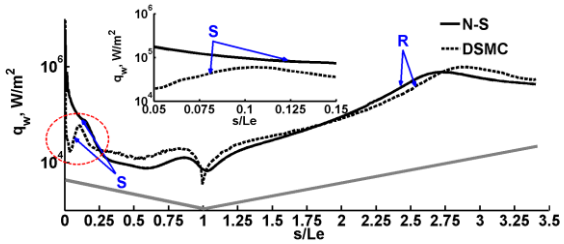

c) Surface heat flux.

Figure 3: Surface parameters.

Chapman's Isentropic Recompression Theory

Chapman's isentropic recompression theory has presented a simple way of finding p_d (also known by Chapman as the dead-air pressure) from the flow condition in the shear layer.

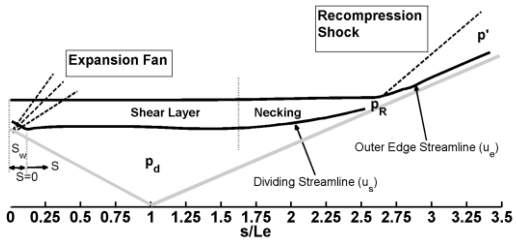

Figure 4: Structure of the shear layer.

As seen from figure 4, the dividing streamline, which delineates the reverse flow region from the downstream flow in the shear layer, has a velocity u_s and the external to the shear layer is u_e.

If the recompression happens isentropically at **R**, the static pressure (p_d) in the recirculation region is related to total pressure (p_t) by the expression given by [2]:

$$p_d = \frac{p'}{\left(1+\frac{\gamma-1}{2}\bar{M}^2\right)^{\frac{\gamma}{\gamma-1}}} \qquad (1)$$

Where $\bar{M}$ is the Mach number on the dividing streamline.

The isentropic assumption implies that p_t equals to the terminal static pressure downstream of the recompression shock (p') and the pressure at reattachment (p_R). However, the current simulations show that for hypersonic flow separation, p_R is not equal to p' as Chapman assumes but the latter is somewhat less. Chapman attributes such a state of affair to the "efficiency of recompression" and viscous effects, both of, which are accentuated in hypersonic flows. This is illustrated in figure 5. In the present results, it is noticed that the fluid is not almost at rest or constant pressure, but the pressure rather starts steadily increasing over most of the compression surface. It is only steady immediately after separation up to the vicinity of the corner vertex. Figure 5 also shows the isentropic and non-isentropic parts of the actual recompression process. It is further noted that there is a further pressure "overshoot" above p'. This is due to the phenomenon of "necking" of the shear layer indicated schematically in figure 4. This is a characteristic of hypersonic shear layers at reattachment. It is known that in hypersonic boundary layers, the subsonic sub-layer (and hence the sonic line) is infinitesimal in thickness [1]. As a consequence, compression waves originating at the reattachment coalesce rapidly in the near vicinity of the reattachment surface. They also make very shallow angles with respect to the streamlines, thus forming the neck. The result is an over-shoot in pressure p_p as indication in figure 5.

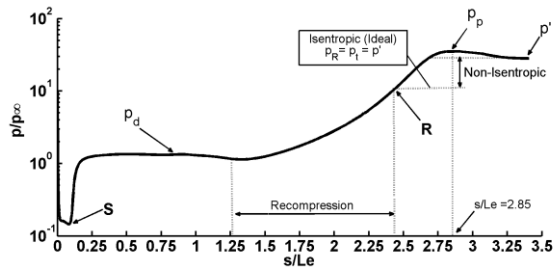

Figure 5: Hypersonic recompression for the "tick" configuration.

Figure 6 shows the variation of the normalized velocity u_* at the dividing streamline with respect to the separation distance S^*. S^* is defined as the normalized streamline distance with S being the streamwise distance from **S,** and S_w the shear function defined in [2].

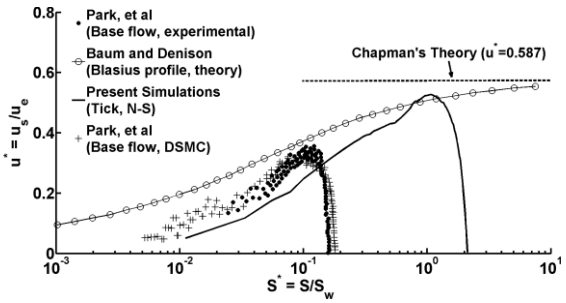

Figure 6: Variation of velocity distribution along the shear layer.

According to Chapman's theory, u_* on the dividing streamline remains constant and independent of Re_∞ or M_∞ [2]. Figure 6 shows the profile for u_* from the current simulations and experimental/numerical studies of Baum and Denison [2] on base flow under the same flow conditions [11]. The profiles show a clear deviation from Chapman's constant velocity assumption. Also shown is Baum and Denison's profile, which assumes a Blasius boundary layer prior to separation so that u_* asymptotes to Chapman's theoretical value (0.587) in the limit of $S^* \to \infty$. In the case of both base flow and leading edge separation cases, such asymptotic behavior is not evident. Instead u_* begins to decrease rapidly soon after reaching a peak.

The maximum u_* for current simulations was found to be higher (0.526) than the experimental results of the base flow (0.356).

The implications of the data from figure 6 is that for finite configurations the viscous dominated separation process is Re_∞ dependent, and the higher the Re_∞, the larger the separation length. However, at the present time, this conclusion is only tentative.

Table 5 shows the difference between p_d/p' calculated from equation (1) and the average p_d/p' extracted from the pressure curve in figure 5.

Parameter	Isentropic	N–S
u_* (Maximum)	0.587	0.526
p_d/p' (Average)	0.334	0.156

Table 5: Comparison between Chapman's theory and average numerical data.

Streamline Angles at Separation and Reattachment

The simulations allowed the calculation of streamline angles at separation (θ_S) and reattachment (θ_R) using the theoretical expression given by Oswatitsch [9]. Through computer values of the pressure gradient ($\partial p/\partial x$) and the shear stress gradient ($\partial \tau/\partial x$) at **S** and **R**, the results are then compared with the measured streamline emanating from **S** and **R** (Figure 7)**.** The results are given in table 6, and show a better agreement at **R** than **S.** A reason for that could be due to the rapid change in the curvature of the streamline at **S** compared to that on **R**.

$$\theta = tan^{-1} - 3\frac{\partial \tau/\partial x}{\partial p/\partial x} \qquad (2)$$

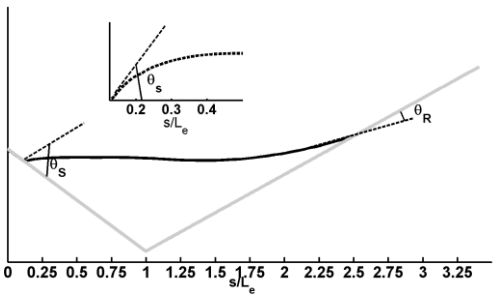

Figure 7: Streamline angles at separation and reattachment**.**

Angle	Theory	Measured
$\boldsymbol{\theta_S}$	30.3	46
$\boldsymbol{\theta_R}$	6.7	8

Table 6: Theoretical and measured streamline angles in degrees.

Conclusions

Hypersonic flow separation at moderately high-enthalpy and moderately low Reynolds number over a "tick" configuration was considered for a numerical investigation using a N–S solver. For code verification, results were compared to a parallel study using the DSMC simulations. In general, the comparison showed good agreement between the N–S and DSMC solvers. Evidence for this agreement was seen in the consistent predictions of surface parameters such as shear stress, pressure, and heat flux. Another verification of the agreement was in locating separation and reattachment, which define the size of the separation bubble. In addition, in the present results, some features characterizing hypersonic flow separation were found to be consistent with those of previous studies. First was the peak location of surface parameters, was seen to occur downstream of reattachment. Second was the pressure of "necking" in the reattachment region.

Another important aspect of the study was to test the applicability of Chapman's isentropic recompression theory under hypersonic conditions. The results have shown that Chapman's theory did not perform as good as at the moderate flow conditions studied previously. For example, the dividing streamline velocity in the shear layer was no longer constant as indicated in Chapman's theory. Chapman's theory has over-predicted the average dead-air pressure by a factor of nearly 2.

Finally, streamline angles at separation and reattachment were compared to Oswatitsch's theoretical formula. Results have shown a better agreement between the measured and calculated values in predicting the reattachment angle. The separation angle, on the other hand, showed a larger discrepancy between the measured and theoretical predictions.

References

[1] Babinsky, H. and J.K. Harvey, *Shock Wave-Boundary-Layer Interactions*. Vol. 32. 2011: Cambridge University Press.

[2] Baum, E. and M.R. Denison, *Compressible Free Shear Layer with Finite Initial Thickness.* AIAA Journal, 1963. **1**(2): p. 342-349.

[3] Chapman, D.R., et al., *Investigation of Separated Flows in Supersonic and Subsonic Streams with Emphasis on the Effect of Transition*. 1958, NACA.

[4] Deepak, N., et al., *High-Enthalpy Flow Over a Rearward Facing Step – A Computational Study.* Journal of Fluid Mechanics, 2012. **695**: p. 405-438.

[5] Hruschka, R., et al., *Comparison of Velocity and Temperature Measurements with Simulations in a Hypersonic Wake Flow*, in *Experiments in fluids*. 2012. p. 407-421.

[6] Jacobs, P.A., et al., *Eilmer's Theory Book: Basic Models for Gas Dynamics and Thermochemistry.* Mechanical Engineering Report, 2010. **9**.

[7] Mallinson, S.G., et al., *The Interaction of a ShockWave with a Laminar Boundary Layer at a Compression Corner in High-Enthalpy Flows Including Real Gas Effects.* Journal of fluid mechanics, 1997. **342**: p. 1-35.

[8] Moss, J.N., et al. *Simulations of Hypersonic High-Enthalpy Separated Flow Over a "Tick" Configuration*. in *28th International Symposium on Rarefied Gas Dynamics*. 2012. AIP Publishing.

[9] Oswatitsch, K., *The Conditions for the Separation of Boundary Layers*, in *Contributions to the Development of Gasdynamics*. 1980, Springer. p. 6-18.

[10] Park, G., et al., *Laminar Near Wake of a Circular Cylinder at Hypersonic Speeds.* AIAA journal, 2010. **48**(1): p. 236-248.

[11] Park, G., et al., *Hypersonic Base Pressure Behind a Blunt Body Using an Isentropic Recompression Model*. 2012.

[12] Roache, P.J., *Fundamentals of Verification and Validation*. 2009: Hermosa Publ.

[13] Wada, Y. and M.-S. Liou, *An Accurate and Robust Flux Splitting Scheme for Shock and Contact Discontinuities.* SIAM Journal on Scientific Computing, 1997. **18**(3): p. 633-657.